Zero-voltage states in ac-driven long Josephson junctions

Niels Grønbech-Jensen
Department of Applied Physics, Stanford University, Stanford, California 94305
and Theoretical Division and Advanced Computing Laboratory, Los Alamos National Laboratory, Los Alamos, New Mexico 87545
(Received 3 September 1991)

Magnetic coupling to long Josephson junctions is analyzed by use of a recently proposed model. The model is discussed in detail, and for a specific geometry of the system we are able to make analytical predictions of zero-voltage steps in the I-V characteristic of the junction embedded in an ac magnetic field. Good agreement is found when comparisons are made to numerical experiments performed on the nonsimplified system.

I. INTRODUCTION

Phase locking of fluxon motion in long Josephson junctions (LJJ's) to external fields has been extensively investigated from a theoretical point of view during the past few years.[1-6] Mainly the study has been done assuming the external field (electric or magnetic) to enter the system through the boundary conditions only. However, as was demonstrated in Refs. 6 and 7 an external magnetic field can in some cases enter the system dynamics of the interior of a LJJ as well. In fact it was demonstrated that the interaction between a LJJ and an external magnetic field could take place for an annular LJJ, which has no open boundaries, and phase locking of fluxon motion to the frequency of the external signal was predicted theoretically, by use of a standard perturbation method.

A similar system has been studied numerically,[8,9] but there the spatial structure of an *electric*- field interaction with the LJJ was combined with *open* boundaries, through which *no* interaction with the external field took place. Although the physical reasons, made in Refs. 8 and 9 for choosing the spatial modulated interaction were not clear, we find many similar features between the numerical results made in Refs. 8 and 9 and the study made in Ref. 6 as well as the study made in this paper. In particular, we will here investigate the phenomenon of zero-voltage steps in the current voltage (I-V) characteristics of a LJJ driven in the one-fluxon mode by a spatial modulated ac force. This is done by analyzing the fluxon dynamics in the annular LJJ coupled to an external ac *magnetic* field. From a standard perturbation approach to the problem, we find that the spatially modulated ac force can provide the fluxon with an effective dc potential well, in which the fluxon is trapped; and thus, even if a dc force is applied, the system will respond with a zero voltage. This is the essential physics in the understanding of the phenomenon. The results presented in this paper are based on several assumptions in order to keep the analysis simple and illustrative. In particular, we have assumed that the geometry of the junction is annular in order to make the spatial modulation of the ac force sinusoidal in space. However, we note that *any* spatial modulation of ac forces acting on the system give rise to similar effects as the ones presented here. Also we note that the choice of boundary conditions is made to keep the analysis simple. Changing the boundary conditions may change the results quantitatively, but will not change the existence of the reported phenomena (see Refs. 8 and 9).

The paper is structured as follows. In Sec. II we will emphasize the model of magnetic coupling and make it clear when and why we can expect spatially modulated perturbations to the LJJ from an external *magnetic* field. In Sec. III we will set up the perturbation method used in this paper. This method takes into account the resonances of the linear modes induced by the magnetic field and is thus a modification to the perturbation treatment made in Ref. 6. In this section we give an analytical explanation for the existence of zero-voltage steps in the I-V characteristics of the ac-driven LJJ and it is analytically demonstrated how the limit cycles of the fluxon mode is uniquely connected to the existence of zero-voltage steps. This is in close agreement with the extensive study of limit cycles made in Refs. 8 and 9. In Sec. IV we show some results of numerical experiments and discuss the validity and limitation of the applied perturbation method. The agreement between the perturbation results and the results of the numerical experiments shows good agreement in the appropriate limits of parameters. Finally, in Sec. V, we will make some conclusions.

II. THEORY

As in Ref. 6 we consider the Lagrangian density $L(x)$, defined by

$$L(x)=\tfrac{1}{2}\phi_t^2-\tfrac{1}{2}\phi_x^2-(1-\cos\phi)+\Delta(\mathbf{B}\cdot\mathbf{n})\phi_x \ , \qquad (1)$$

where x and t are the space and time dimensions normalized to the Josephson penetration depth λ_J and the inverse plasma frequency ω_p^{-1}, respectively.[10] The field ϕ represents the quantum-mechanical phase difference between the two superconductors defining the LJJ and $\mathbf{B}$ is the external magnetic field normalized to $\hbar/2ed\lambda_J$, where $d=2\lambda_L+t_{ox}$, λ_L being the magnetic penetration depth of the superconductors and t_{ox} being the thickness of the insulating layer separating the superconductors. The spatial orientation of the magnetic flux density (ϕ_x) of the

LJJ is represented by the unit vector $\mathbf{n}$, and finally the coupling strength between the LJJ and the external magnetic field is given by the dimensionless parameter Δ. From Eq. (1) we see that, in order to have any interaction, $\mathbf{B}$ needs to have a component in the plane of the barrier of the junction ($\mathbf{B}\cdot\mathbf{n}\neq 0$). Also we observe that if $\mathbf{n}\cdot\mathbf{B}<0$ the system increases its potential energy, whereas if $\mathbf{n}\cdot\mathbf{B}>0$ the system decreases its potential energy.

From the Lagrange density Eq. (1) we get the equation of motion for the phase difference:

$$\phi_{xx}-\phi_{tt}-\sin\phi=(\partial/\partial x)(\Delta\mathbf{B}\cdot\mathbf{n}) , \tag{2}$$

as well as the total energy H of the system:

$$H=\int[\tfrac{1}{2}\phi_x^2+\tfrac{1}{2}\phi_t^2+1-\cos\phi-\Delta(\mathbf{B}\cdot\mathbf{n})\phi_x]dx , \tag{3}$$

where the integral is over the size of the system. If we denote the system length by L, make the time derivative of the system energy, and use Eq. (2) we get

$$dH/dt=(1-\Delta)\phi_x\phi_t|_0^L , \tag{4}$$

where ϕ_x at the boundaries is identical to the external magnetic field $\mathbf{B}\cdot\mathbf{n}$ at the same points.[10] Thus we note that in order to maintain the system as a Hamiltonian system, we must require that the coupling parameter satisfies the conditions

$$\Delta(x=0)=\Delta(x=L)=1 . \tag{5}$$

This choice of the coupling parameter at the boundaries does of course not say anything about the behavior of the coupling parameter in the interior of the junction ($0<x<L$), but it makes it plausible to regard the additional potential-energy term in Eq. (1) as physically relevant, since the undriven and lossless LJJ embedded in a dc magnetic field maintains its conservation of energy.

Interaction between the LJJ and external magnetic field may be obtained in several ways. Of course we may consider the conventional way of applying the field through open boundary conditions, but if the quantity $\Delta\mathbf{B}\cdot\mathbf{n}$ varies along the x direction, we have an influence through the right-hand side of Eq. (2). We can imagine either of the three quantities to be dependent on the x coordinate, but a simple way of realizing a system is to consider the annular LJJ in a spatially homogeneous magnetic field and a coupling parameter $\Delta=1$. In this way we also avoid any open boundary conditions, through which the magnetic field may interact. Of course, we cannot expect the magnetic field to be spatially homogeneous around the superconducting films, but in order to keep the system mathematically simple, we will make this assumption. Including the usual perturbations of energy input and dissipation we now have the system

$$\phi_{xx}-\phi_{tt}-\sin\phi=Bk\sin(kx)+\alpha\phi_t-\eta , \tag{6}$$

where the boundary conditions are given by the annular geometry:

$$\phi(x=0)=\phi(x=L)+2\pi l , \tag{7}$$

l being the total number of trapped flux quanta in the LJJ. Further, it has been assumed that the geometry of the LJJ gives

$$\Delta\mathbf{B}\cdot\mathbf{n}=B\cos(kx) , \tag{8}$$

provided $\Delta=1$. Here $k=2\pi/L$ is the spatial wave number of the system. In Eq. (6) the parameter α represents the normalized loss due to tunneling quasiparticles and the parameter η represents the normalized external bias current density forced through the junction.[12]

III. PERTURBATION THEORY

In order to analyze the one-soliton dynamics ($l=1$) in the perturbed sine-Gordon (PSG) system given by Eqs. (6) and (7) we will make use of the method of separating the soliton field ψ from the field of the externally induced (linear) modes ϵ (Ref. 11)—thus writing $\phi=\psi+\epsilon$. In this way we may preserve information about the resonances of the linear modes, which is important when we consider spatially modulated systems. Making the usual assumption of small perturbations (α,η, and Bk small), we may assume that the magnetic-field-induced mode ϵ is given by the linear equation

$$\epsilon_{xx}-\epsilon_{tt}-\epsilon=\alpha\epsilon_t-\eta-Bk\sin(\Omega t)\sin(kx) , \tag{9}$$

where we have included the time oscillation of the magnetic field. This equation can easily be integrated to give

$$\epsilon=kB\frac{\sin(\Omega t+\Theta)\sin(kx)}{\sqrt{(\Omega^2-k^2-1)^2+(\Omega\alpha)^2}}+\eta ,$$

$$\tan\Theta=\frac{\Omega\alpha}{1+k^2-\Omega^2} . \tag{10}$$

The soliton field is then governed by the equation

$$\psi_{xx}-\psi_{tt}-\sin\psi=\alpha\psi_t-2\epsilon\sin^2(\psi/2) , \tag{11}$$

where ϵ is given by Eq. (1) and $|\epsilon|$ is assumed to be small. Defining the energy of the unperturbed soliton field [left-hand side of Eq. (11)] to be

$$H=\int_0^L(\tfrac{1}{2}\psi_x^2+\tfrac{1}{2}\psi_t^2+1-\cos\psi)dx , \tag{12}$$

and introducing the unperturbed kink-soliton profile

$$\psi^0=4\tan^{-1}[\gamma(u)(x-\xi)] , \tag{13}$$

where ξ is the soliton position, $u\equiv\dot{\xi}$ is its velocity, and $\gamma(u)=(1-u^2)^{-1/2}$ is the inverse Lorentz contraction of the kink, we will make the assumption that the system is long compared to the size of the kink—i.e., that

$$\int_0^L(\cdots)dx\approx\int_{-\infty}^{\infty}(\cdots)dx . \tag{14}$$

This approximation makes the soliton travel in an infinitely long system with the spatial modulation given by k. In this way we do not consider an annular system, since that would require taking into account an infinite sequence of solitons as well. However, for reasonably long systems this approximation is quite good (see, e.g., Refs. 6 and 7). Inserting the kink profile Eq. (13) into the energy expression Eq. (12) and using the approximation of Eq. (14) we find in the framework of the well-known

adiabatic perturbation method[12] the dynamical equation for the collective coordinate ξ in the form

$$dH/dt = -8\alpha u^2\gamma(u) - 2\pi\eta u - 2\pi u k B\Gamma \sin(\Omega t)\sin(k\xi) , \tag{15}$$

where we have defined the quantity Γ by

$$\Gamma = \frac{1+k^2(1-u^2)}{\sqrt{(1+k^2-\Omega^2)^2+(\Omega\alpha)^2}} \operatorname{sech}\left[\frac{\pi k}{2\gamma(u)}\right] , \tag{16}$$

and where

$$H = \frac{8}{\sqrt{1-\dot{\xi}^2}} \tag{17}$$

for the soliton.

From Eq. (15) we see that the soliton motion may resonate with the external frequency Ω in many different ways and hereby cause phase-locked steps in the *I-V* characteristics of the junction at soliton frequencies (voltages) given by $\omega=(m/n)\Omega$. In particular, we note the phase locking at the fundamental frequency Ω, which was also predicted in Ref. 6 by using a simpler perturbation method, not taking into account the dispersion relation of the linear mode. The condition for phase locking at the fundamental frequency is that the change, ΔH, in the soliton energy during one period of the driving field $2\pi/\Omega$ is zero—i.e., that

$$\Delta H = \int_0^{2\pi/\Omega} \frac{dH}{dt} dt = 0 . \tag{18}$$

This integral is easily evaluated if we assume that the soliton travels through the system with constant velocity

$$u_0 = \pm\frac{\Omega L}{2\pi} = \frac{\Omega}{k} , \quad \xi_0 = u_0 t + \frac{\Theta_0}{k} , \tag{19}$$

where Θ_0 is a phase angle. By adjusting this angle we may obtain the total phase-locking range $\delta\eta$ of this mode to be

$$\delta\eta = \frac{kB}{\sqrt{1+[\Omega\alpha/(1+k^2-\Omega^2)]^2}} \operatorname{sech}\left[\frac{\pi k}{2\gamma(\Omega/k)}\right] . \tag{20}$$

Equation (20) predicts a symmetric step around the *I-V* curve for the system with no magnetic field applied to it. This result is slightly different from the one obtained in Ref. 6, where the square root in the denominator was absent. However, realizing that all perturbations must be small ($\alpha \ll 1$) and that driving frequency must be less than the spatial wave number ($\Omega < k$) in order to be able to obtain phase locking of the soliton motion at the fundamental frequency, we find that this correction of the predicted locking range[6] can be neglected. This is reasonable, since very good agreement between the results of numerical experiments and the prediction made in Ref. 6 were found. We note that if phase locking at other frequencies than the fundamental were to be studied, the dispersion relation of the linear mode can prove to be much more important. This will be reported elsewhere.[13]

If we now assume that the soliton moves with nonrelativistic velocity ($\dot{\xi}^2 \ll 1$) we may write the dynamical equation for the collective coordinate in the following way:

$$\ddot{\Phi} = -\alpha\dot{\Phi} - \frac{\pi k}{4}\eta - \frac{\pi k}{4} kB\Gamma \sin(\Omega t+\Theta)\sin(\Phi) , \tag{21}$$

where we have introduced the phase angle $\Phi = k\xi$. This equation clearly describes a parametrically driven particle. Following Ref. 14 we can regard the frequency of the external drive to be much faster than the average soliton motion. Under this assumption, we may write the variable $\Phi = \Psi + \zeta$ as a sum of a slowly varying component (Ψ) and a fast oscillating component (ζ) with zero mean. The rapidly oscillating component is considered to be of small amplitude ($|\zeta| \ll 1$). Inserting this separation into Eq. (21) and separating the terms oscillating with the frequency Ω we get

$$\ddot{\zeta} = -\alpha\dot{\zeta} - \frac{\pi k}{4} kB\Gamma \sin(\Psi)\sin(\Omega t+\Theta) \tag{22}$$

$$\Rightarrow \zeta = -\frac{\pi k}{4}\frac{kB}{\Omega^2+\alpha^2}\Gamma \sin(\Psi)\left[\sin(\Omega t+\Theta) + \frac{\alpha}{\Omega}\cos(\Omega t+\Theta)\right] . \tag{23}$$

Similarly we separate the slow "dc" terms yielding

$$\ddot{\Psi} = -\alpha\dot{\Psi} - \frac{\pi k}{4}\eta - \frac{\pi k}{4} kB\Gamma \cos(\Psi)\langle \zeta \sin(\Omega t+\Theta)\rangle , \tag{24}$$

where the bracket denotes the time average. This equation can then be rewritten in the form

$$\ddot{\Psi} = -\alpha\dot{\Psi} - \frac{\pi k}{4}\eta - \left[\frac{\pi k}{8} kB\right]^2 \frac{\Gamma^2}{\Omega^2+\alpha^2}\sin(2\Psi) . \tag{25}$$

Equation (25) has the form of an effective (slow-motion) pendulum equation in 2Ψ, where the effective harmonic potential is induced by the "fast" oscillating parametric force acting on the collective coordinate particle. As is obvious from this "slow motion" equation, we can apply a finite external bias current η and still maintain the soliton trapped in the induced potential well. This bias is given by

$$|\eta| < \frac{\pi k}{16}\left[\frac{kB}{\Omega^3}\right]^2 \frac{1}{1+(\alpha/\Omega)^2} \times \frac{(1+k^2)^2}{[1+(k/\Omega)^2-(1/\Omega)^2]^2+(\alpha/\Omega)^2} \operatorname{sech}^2\left[\frac{\pi k}{2}\right] . \tag{26}$$

Clearly this limit is in itself an upper limit, since the expression does not take the fast oscillations into account. These oscillations will decrease the height of the actual zero-voltage step because the energy stored in the vibrating motion Eq. (23) will make the particle move out of the potential well for lower values of η than predicted by Eq. 26. Actually, we can calculate the vibration energy

of the motion Eq. (23) and estimate that the size of the zero-voltage step is $2\sqrt{2}/3 \approx 0.94$ times the prediction made in Eq. (26).

From Eqs. (23) and (25) we are able to construct the limit cycle of the fluxon analytically. Inserting the static fix point Ψ_* of Eq. (25)

$$\Psi_* = -\frac{1}{2}\sin^{-1}\left[\frac{\Omega^2+\alpha^2}{\Gamma^2}\frac{16}{\pi k}\frac{\eta}{k^2B^2}\right] \tag{27}$$

into Eq. (23), we obtain the limit cycle in the phase plane $(\zeta,\dot{\zeta})$ for the collective coordinate as an elliptic motion with the period of the external drive $(2\pi/\Omega)$. From the expressions above it is evident how the dynamics of the system creates a certain amplitude of the limit cycle $(\zeta,\dot{\zeta})$ determined by Eqs. (27) and (23). Then from Eq. (24) we see how the dynamics of the system seeks to react by creating a "dc potential" proportional to the spatial amplitude of the limit cycle.

IV. NUMERICAL EXPERIMENTS

In order to verify the condition Eq. (26) for obtaining the zero-voltage step in the annular junction, we have performed numerical experiments on the system defined by Eqs. (6) and (7) for different values of system length L, magnetic-field amplitude B, and the driving frequency Ω. The numerical method for integrating the field equation was chosen to a second-order finite-difference method in time and a fourth-order finite-difference method in space. The integration step sizes in time and space were varied and chosen pending the actual parameters. For simplicity we have in all our numerical experiments chosen the dissipation parameter to be $\alpha=0.1$.

In Fig. 1 we show a section of a normalized I-V curve for a system defined by the parameters $L=10$, $\Omega=0.8k$, and $kB=0.2$. Clearly we observe the phase-locked step at the fundamental frequency $\omega=\Omega$ as well as many subharmonic steps at frequencies $\omega=(m/n)\Omega$ (the five largest subharmonic steps are indicated in the figure). More important for this paper, however, is to observe that the dc I-V curve has a step for zero voltage $(\omega\equiv 0)$. This step is in fact the second largest step—only dominated by the step at the fundamental frequency $(\omega=\Omega)$. We note that the zero-voltage step is actually twice the size of what is shown in Fig. 1, since the I-V curve continues antisymmetrically for negative η values.

In Fig. 2 we have shown the comparison between the perturbation result Eq. (26) (solid curve) and numerical experiments (markers). We have here chosen the driving frequency to $\Omega=k$ and we have plotted the (half) size of the zero-voltage step as a function of the magnetic field B. Clearly, we see that the predicted quadratic dependence on the external magnetic filed is fulfilled in the interval of the chosen amplitudes for both system lengths ($L=10$ and 20). As noted above, the predicted step size of Eq. (26) is an upper limit to what we might expect from the numerical experiments, so the trend found in Fig. 2(a) that the numerical experiments show a smaller step than predicted does not come as a surprise and we note that the error of the predicted size compared to the

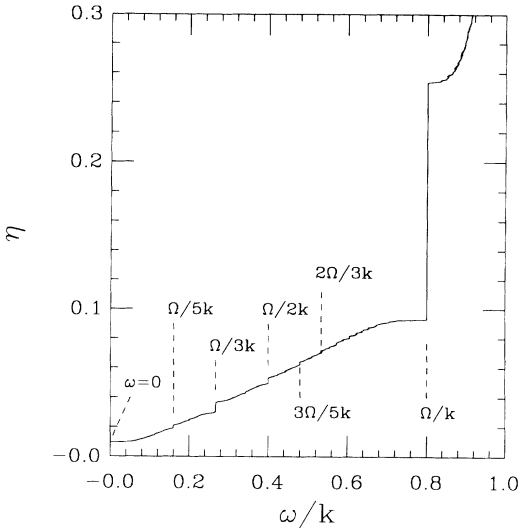

FIG. 1. Normalized I-V curve calculated from the field equation Eq. (6). Parameters are $L=10$, $kB=0.2$, $\Omega=0.8k$, and $\alpha=0.1$. The step at the fundamental frequency Ω is indicated together with the five most significant steps at subharmonic ratios of the drive as well as the zero-voltage step.

measured is less than 20%. For $L=20$ [Fig. 2(b)] we find that the comparison in general is better—apart from the high values of the magnetic-field amplitude. The trend that the longer systems show better agreement than the shorter is of course an artifact of the assumptions made in the perturbation treatment. First we note that the approximation mentioned in Eq. (14) is closer to reality when the system is long. Second, we note that the equation for the linear mode Eq. (9) is considered in a system without a trapped soliton. Thus, the resulting standing wave, driving the soliton, is idealized with respect to resonances, since the soliton, with its finite width, will perturb the linear mode field and then suppress the resonance described by Eq. (11) for the shorter systems. In general we may expect a suppression of the resonance for all system lengths, since the perturbation treatment has information of the *linear* mode ϵ only. Of course, when the resonance is reached, the amplitude of the ϵ field is predicted to be $kB/\Omega\alpha$, which may be a large number, and thus outside the validity of Eq. (11). [The violation of the linear assumption is also the reason for the deviation between the analytical curve and the experimental data for "large" B in Fig. 2(b).]

This suppression of the predicted resonance is visible in Fig. 3, where we have shown the comparison between the perturbation results and the numerical experiments for the zero-voltage step size as a function of the driving frequency Ω. Clearly we find that the agreement between the experiments and the perturbation treatment is very good as long as the driving frequency is not too close to the predicted resonance. In spite of the discrepancy near the resonance, we do find a peak in the experimental data for frequencies $\Omega \approx (1+k^2)^{1/2}$, indicating that the linear mode does in fact resonate near the predicted frequency—although this is not a quantitatively correct result. Closer agreement between the results of the numerical experiments and the perturbation result could be

obtained if the presense of the soliton were taken into account in the equation for the linear mode Eq. (9) and if the nonlinearity of the ϵ field were maintained in the description. For driving frequencies larger than the resonance, we find that the agreement is again better and we may then predict that zero-voltage steps will not be observable in real junctions for driving frequencies significantly larger than the resonance frequency of the linear mode, since the perturbation result shows that the step size will decrease as $\sim\Omega^{-6}$. It is instructive to note that the perturbation result seems to agree with the numerical data even for low frequencies, albeit it is derived under the assumption of a "fast" oscillating field. Actually we find reasonably good agreement down to $\Omega \approx k/4$,

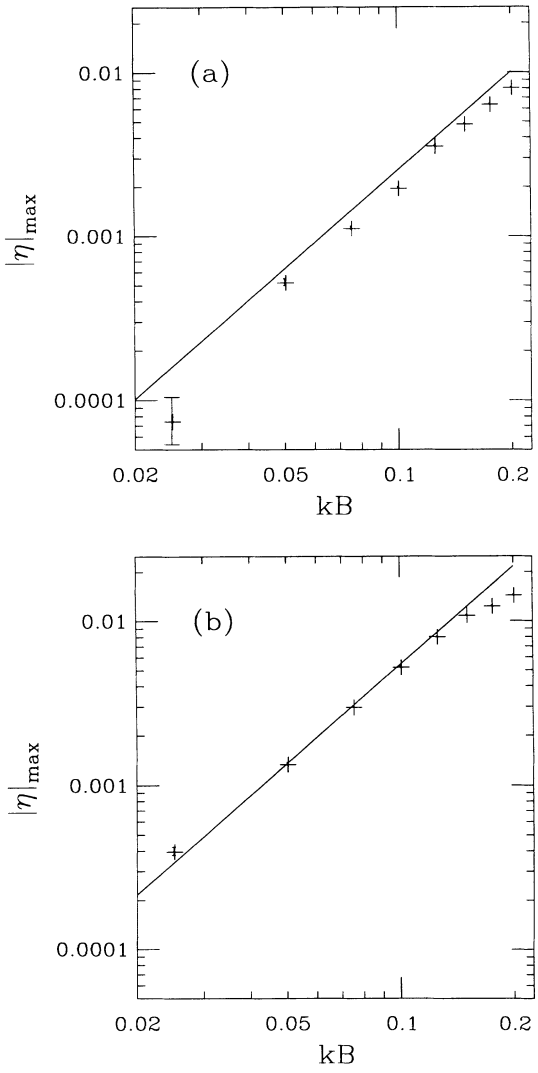

FIG. 2. The size of the zero-voltage step as a function of the applied amplitude kB. The solid line represents the analytical prediction Eq. (26) and the markers represent the results of the numerical experiments. The estimated error is in most cases less than the size of the markers. If bigger, the result is indicated by an error bar as well. Parameters are $\alpha=0.1$, $\Omega=k$, (a) $L=10$, (b) $L=20$.

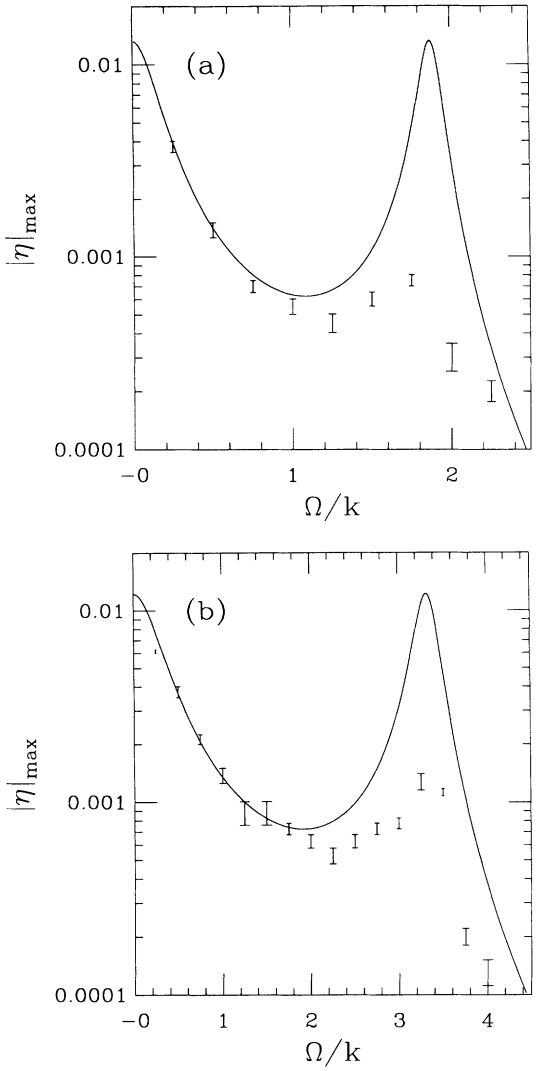

FIG. 3. The size of the zero-voltage step as a function of the applied frequency Ω. The solid line represents the analytical prediction Eq. (26) and the error bars represent the results of the numerical experiments. Parameters are $\alpha=0.1$, $kB=0.05$, (a) $L=10$, (b) $L=20$.

which is a quite low frequency. The real understanding of the term "fast" must here be considered the following: The period of the driving field should be much smaller than the time it takes for the soliton to circulate the junction ones with the applied dc bias η. This means that even if the above prediction of the size of the zero-voltage step does not hold for very low frequencies, we can obtain a zero-voltage step with smaller size.

V. CONCLUSION

An analytical prediction of zero-voltage steps, and their sizes, in the I-V characteristics of an annular Josephson junction coupled to an external ac magnetic field has been given. Comparisons to numerical experiments have shown very good quantitative agreement in the expected parameter regions, and qualitative agree-

ment is found when the system is operated near the resonance of the linear mode, induced by the external magnetic field. Hence, we have found that zero-voltage steps may in fact exist in LJJ's driven by spatially modulated ac forces. It is interesting to make the parallel to the zero-voltage steps reported in Ref. 7, where a dc magnetic field created a potential well for the soliton. In the dc case it was found that the zero-voltage step size increased as $\sim B$ and the soliton motion were periodic with the length L, whereas we have found in this paper that the ac field created a zero-voltage step of size $\sim B^2$ and a soliton motion periodic with $L/2$.

The work presented in this paper can be related to the numerical study[8,9] of a long Josephson junction with *open* boundary conditions and a spatially modulated ac *electric* field acting on the system. There zero-voltage steps were also observed and we believe that the zero-voltage phenomenon reported in Refs. 8 and 9 and the zero-voltage steps predicted in this paper are created by the same mechanism—an effective dc potential, induced by the spatially modulated ac driving field, which acts as a parametric force on the collective coordinate particle in the reduced system. More specifically, we have demonstrated analytically how the limit cycles of the fluxon mode uniquely is connected to the existence of the zero-voltage steps. However, the step size predicted in this paper will most probably not apply to the system with open boundary conditions, since the soliton experiences reflection losses and phase shifts during reflections (see, e.g., Ref. 2 for details) at the boundary. In particular the reflection losses make a difference between the system considered here and the system studied in Refs. 8 and 9, since reflecting boundary conditions require an oscillating mode of the soliton in order to avoid annihilation of the soliton. Thus, a mode of $\eta=0$ does not exist for reflecting boundary conditions, as also noted in Refs. 8 and 9.

Some remarks can be made about the idealized system discussed in this paper. As noted in the Sec. II, we cannot expect a perfect homogeneously magnetic field around a superconductor. Further, we may expect that the junction provides some spatial variation of the coupling parameter Δ as a function of x, and finally we may consider other geometries of the function than the annular. We note, however, that any periodic structure in the modulation of the system will give rise to phenomena similar to the ones described in this paper and further, we note that the perturbation treatment presented here easily (in principle) can be generalized to any periodic structure of the form

$$\frac{\partial}{\partial x}(\Delta\mathbf{B}\cdot\mathbf{n})=\sum_n [a_n(t)\sin(knx)+b_n(t)\cos(knx)] , \qquad (28)$$

and hence, we may consider more complicated structures of the spatial modulation. We note finally that long annular Josephson junctions are well within current fabrication capabilities.[15–17] Measurements have been made on these systems containing one or more solitons. Experiments are currently being prepared[18] in order to verify the bifurcation and phase-locking phenomena described in Refs. 6 and 7 as well as the zero-voltage steps described in this paper.

ACKNOWLEDGMENTS

The author acknowledges many useful discussions with Peter S. Lomdahl and Mogens R. Samuelsen as well as Yuri S. Kivshar, Boris A. Malomed, Mario Salerno, and Robert D. Parmentier. Also the author is grateful to the Otto Mønsteds Fond and the Carlsberg Fondet for financial support during the initial and final part of this work, respectively. We thank the Los Alamos Advanced Computing Laboratory for generous support and for making their facilities available to us. Part of this work was performed under the auspices of the U.S. Department of Energy.

[1]M. Salerno, M. R. Samuelsen, G. Filatrella, S. Pagano, and R. D. Parmentier, Phys. Lett. A **137**, 75 (1989).
[2]M. Salerno, M. R. Samuelsen, G. Filatrella, S. Pagano, and R. D. Parmentier, Phys. Rev. B **41**, 6641 (1990).
[3]M. Salerno, Phys. Lett. A **144**, 453 (1990).
[4]M. Salerno and M. R. Samuelsen, Phys. Lett. A **156**, 293 (1991).
[5]N. F. Pedersen and A. Davidson, Phys. Rev. B **41**, 178 (1990).
[6]N. Grønbech-Jensen, P. S. Lomdahl, and M. R. Samuelsen, Phys. Lett. A **154**, 14 (1991).
[7]N. Grønbech-Jensen, P. S. Lomdahl, and M. R. Samuelsen, Phys. Rev. B **43**, 12 799 (1991).
[8]J. C. Fernandez, R. Grauer, K. Pinnow, and G. Reinisch, Phys. Lett. A **145**, 333 (1990).
[9]J. C. Fernandez, R. Grauer, K. Pinnow, and G. Reinisch, Phys. Rev. B **42**, 9987 (1990).
[10]See, e.g., A. Barone and G. Paterno, *Physics and Applications of the Josephson Effect* (Wiley, New York, 1982).
[11]O. H. Olsen and M. R. Samuelsen, Phys. Rev. B **28**, 210 (1983).
[12]D. W. McLaughlin and A. C. Scott, Phys. Rev. A **18**, 1652 (1978).
[13]Niels Grønbech-Jensen, Boris A. Malomed, and Mogens R. Samuelsen (unpublished).
[14]See, e.g., L. D. Landau and E. M. Lifshitz, *Mechanics,* 3rd ed. (Pergamon, New York, 1976).
[15]A. Davidson, B. Dueholm, B. Kryger, and N. F. Pedersen, Phys. Rev. Lett. **55**, 2059 (1985).
[16]A. Davidson and N. F. Pedersen, Appl. Phys. Lett. **44**, 465 (1983).
[17]A. Davidson, B. Dueholm, and N. F. Pedersen, J. Appl. Phys. **60**, 1447 (1986).
[18]A. Davidson (private communication).